Hybrid-Microgrid Planning, Sizing and Optimization for an Industrial Demand in Pakistan

Zahid JAVID, Ke-Jun LI, Rizwan UL HASSAN, Jian CHEN

Abstract: Industrial sector is of great significance for the economic growth of every country. The energy crisis in Pakistan has become the prime stumbling block in the economic development of the country. There are many industrial processes that need uninterrupted supply; even a trivial outage can cost millions of dollars. The main cause of "load shedding" in Pakistan is that it produces a major portion of its energy from fossil fuels, whose price and demand is constantly increasing. Most of the customers at industrial and commercial level use Diesel Generator (D_iG) as a reliable alternative source of electrical power when grid supply is unavailable. The use of D_iG during loading shedding hours would increase the Cost of Energy (COE) per kWh and also enhance environmental emissions. Pakistan has a wide range of renewable power sources like bioenergy, wind, solar, hydel, geothermal etc. The distinct emphasis on the implementation of an industrial microgrid in Faisalabad, Pakistan has been specified in this paper. The prospective benefits of the microgrid fall into three major kinds: cost reduction, fuel saving, and improved environmental emissions. The optimized objective of this work is to maximize these benefits. Moreover while designing the hybrid microgrid system it encounters many design challenges like sizing of the components, system feasibility, COE, system reliability etc. This study contributes to the ongoing studies about hybrid microgrid system and draws attention to the optimal design and sizing considering several techno-economic factors including Net Present Cost (NPC), COE, supply reliability, capacity shortage constraint, battery state of charge (SOC), dispatch strategy, PV power generation and PV array tracking systems. Different cases are studied; microgrid sizing, techno-economic exploration, sensitivity analysis and environmental effects are addressed using (Hybrid Optimization Model for Electric Renewables) HOMER. The results show that COE and environmental emissions have been significantly reduced for the proposed system.

Keywords: environmental emissions; fossil fuels; HOMER; industrial microgrid; Pakistan energy crisis, renewable resources

1 INTRODUCTION

Pakistan is going through its critical period of power shortage. Energy shortfalls in the last year reached an average of 4.5 GW to 5.5 GW. Electricity demand of the country is increasing with a rate of 8% per year [1].The demand would expectedly climb up to 54 GW by the end of 2020 and 113 GW in 2030 [2]. More than 140 million Pakistanis either have no access to the power grid or suffer over twelve hours of load-shedding every day. Now Pakistan is dependent on imported fossil fuel to generate electricity which is too expensive and also not the suitable choice due to environmental cautions. According to a survey (2015-2016), 64% of the total electricity generation in Pakistan is from fossil fuel. This categorical transferal to fossil fuels thus deduces that the country has seriously compromised on its energy security.

Another downside of fossil fuel is an enormous financial burden. Under all these circumstances Pakistan`s industry has been badly shrunken. Industries are forced to use diesel generators to meet their requirements. Pakistan is among the countries that are abundant with renewable energy sources like solar, wind, geothermal, biogas, micro hydel / canal fall, biodiesel, biomass, tidal/ocean energies etc. To fulfil the demand of industries and rural community, microgrid utilizing renewable energy sources is one of the worthwhile options to overcome the identified problems. [3] discussed the renewable potential present in Pakistan but no efforts were made to harness this potential due to lack of awareness and research in this field. While designing a hybrid microgrid system there are lots of factors that should be considered; the load should be considered very carefully, available resources, sizing of the component, how a new system (microgrid) will coordinate with the old system (conventional system) and its economics etc.

Charline Stevanoni [4] uses games theory to study the planning and profitability of industrial microgrids connected to the distribution network, and have many perspectives such as the dynamic choice of the year for undertaking long-term investments (with proper component sizing). Moein Choobineh [5] proposed a multi-step methodology for emergency operation of an industrial park when the electric utility is not available due to a disturbance and formulated it as a network reconfiguration problem that tries to maximize the amount of load served by reconfiguring the network topology and using backup energy resources. The problem is solved and analyzed for a simplified version of an industrial park, both at steady state and during transients.

Hybrid microgrid planning presents a significant research and engineering challenge and hence needs increased research efforts. The purpose of this study is to find the best combination of renewable energy sources and component sizing from the available resources at a certain site that can meet the electricity demand (industrial demand) in a reliable and sustainable manner and to analyze whether such hybrid option is a cost-effective solution or not. To achieve this objective we chose an industrial load in Faisalabad city for study, estimated the potential demand, and identified the available resources, modeled the system based on multiple combinations of renewable energy technologies (RETs) with the application of HOMER software. The rest of the paper is organized as follows: section 2 is about the literature review and explains the need and significance of this work; section 3 briefly discusses the system under consideration in terms of resources assessment and systems input data, section 4 shows the simulations and results considering different study cases, finally section 5 presents the conclusions of this work.

2 LITERATURE REVIEW

The purpose of the literature survey presented here is twofold: first, this delivers the indication of knowledge gap that authenticates the need for this work; and second, to provide a facility for the methodology used in the study and is a source of information for evaluation, triangulation and referencing.

Performance of microgrid has been studied from different perspectives such as power quality improvement [6], scheduling [7], power management and control [8, 9], and protection [10]. However, few attempts have been made to bring this technology to the industrial and commercial buildings where the reliability and the quality of the supply are mandatory [11-13]. Sinha and Chandel concluded that HOMER is the simpler and fastest tool to evaluate Renewable Energy Technologies RETs [14]. Many researchers have modelled and evaluated hybrid microgrid using HOMER in different perspectives. Givler in [15] directed a case study of Sri Lanka and acknowledged that when a *PV*/diesel hybrid becomes cost-effective compared to the stand-alone small solar home system. However, this study emphasis is on basic needs and does not embrace the productive use of energy.

Omar Hafez [16] investigated the optimum design and planning of renewable energy based microgrid system for a hypothetical rural community. Although the study considers electricity demand over 24 hours, the purely hypothetical nature of the assumptions makes the work naive for many off-grid areas. The results presented in his study show that the Diesel-Renewable Mixed Microgrid (diesel, wind, solar *PV*, battery, micro-hydro, converter) has the lowest Net Present Cost (*NPC* = 10.496 M$) as well as the lowest cost of energy (*COE* = 0.449 $/kWh). Asad Waqar [17] projected a microgrid consisting hydro turbine, biomass generator, diesel generator, *PV* array and batteries to find out the optimal system outline in terms of generation mix and unit sizing with minimum costs (*NPC* = 6.80 M$, *COE* = 0.045 $/kWh). Mashood Nasir presented a system-level design and analysis of a solar photovoltaic (*PV*) integrated building scale hybrid AC/DC microgrid; his proposed architecture minimizes the AC/DC inter-conversion losses by allocating DC power to DC loads and AC power to AC loads via an intelligent power electronic controller [18].

M. Khurram Abbas [19] suggested an economic hybrid energy system (*PV*, diesel, wind) for electrification of an off-grid remote site, named as Rakhi Gaj in Pakistan. The study addressed also the electrical demand for the water pumping station and household's appliance. Jun Zhang & Ke-Jun Li [20] discussed the bi-level program for the planning of an islanded microgrid in terms of compressed air energy storage (CAES). This study proposed a bi-level program to determine the optimal size of D_iG and CAES. Samuel and Wei-Jun Lee documented a case study on microgrid modular design for tribal healthcare facilities with *PV* system [21].

Mamta Suthar [22] evaluated the performance of PV tracking system and proved that the yearly radiation gain by two-axis tracker is 3.7% and 47.3% more with respect to single-axis tracking and fixed horizontal surfaces, respectively. In another study, S. G. Mane [23] showed that Power generated by Dual Axis Solar Tracking System is 26.72% more than the fixed solar panel during the whole observation time period.

It can be seen that hybrid options have often considered a limited set of technologies. Moreover, most studies focused on providing electricity purely for domestic purpose and did not take into account the electricity demand for industrial and small-scale business units especially in Pakistan. The load profiles are also not sensibly considered in many cases. Performance of *PV* system with and without tracking was studied as a separate system but not with hybrid microgrid. These issues are well-thought-out in the present study, thereby linking the knowledge gap. Our contribution arises from six novel features: 1) most of the studies in the past only discussed the energy sources available in Pakistan, there is no such research conducted yet; 2) we conducted a comparative study between fixed angle *PV* panels and with two axis tracking system; 3) the reliability of supply, which has not got a satisfactory consideration in the literature, is considered as a fundamental objective; 4) we have involved best use of electricity in industrial energy needs, thereby expanding the scope of the study; 5) previous studies did not discuss much the bioenergy integration in microgrid and 6) we have considered the actual industrial load profile in the present study.

3 METHODOLOGY

An assessment of the load profile, solar irradiation, air temperature, wind speed and bioenergy availability is conducted at an early stage of this work.
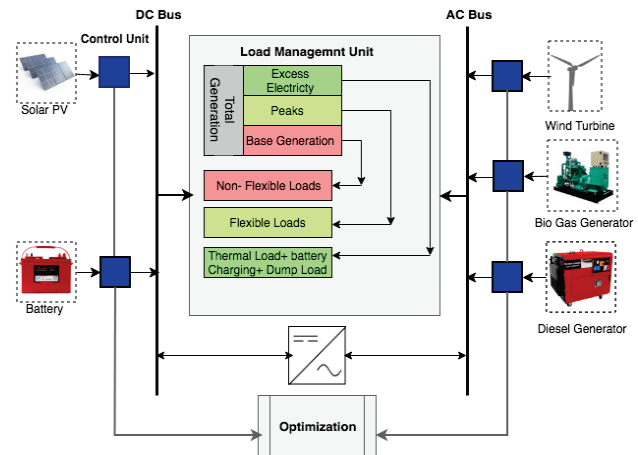

Figure 1 Proposed model

The load is characterized into different categories according to its priority. Non-flexible loads are the loads that need uninterrupted supply and have the highest priority while flexible loads have low priority. It includes deferrable loads and battery charging as shown in Fig. 1. The proposed system optimization model is shown in Fig. 2. After gathering all the necessary data it is fed into HOMER. HOMER generates optimized results in terms of sizing and system configuration with respect to Net Present Cost (*NPC*) subject to defined objective function in Eq.(1) and power balance constraint defined in Eq. (2).

$$O(C) = \min(C_G, C_E) \qquad (1)$$

$$P_{Load}(t) = P_w(t) + P_{pv}(t) + P_{bg}(t) + P_{bat}(t) + P_{DiG}(t) \qquad (2)$$

where C_G is the power generation cost of fuel generators that includes the fuel cost, operation and maintenance cost and emission penalties; C_E is cost of emissions penalties because of fuel generators.
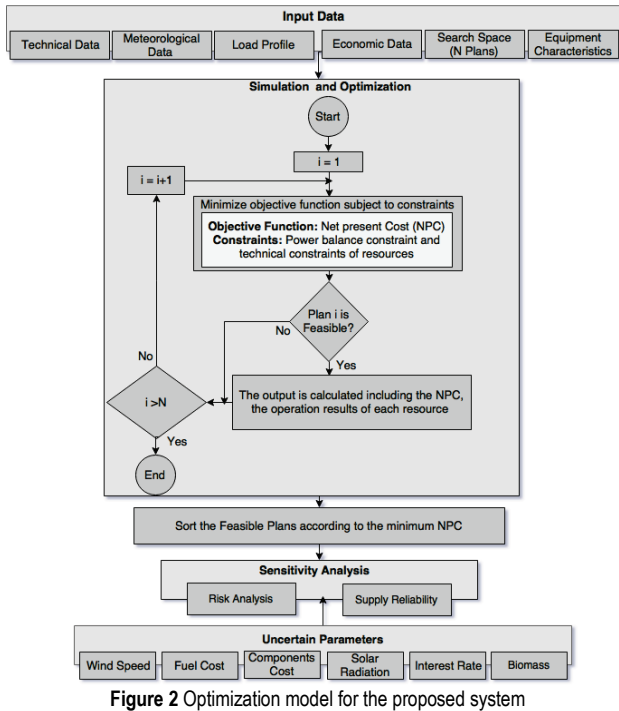
Figure 2 Optimization model for the proposed system

The power generation cost of fuel units can be expressed as:

$$C_{\mathrm{G}} = \sum_{t=1}^{T} \sum_{i=1}^{N} \left[F_{\mathrm{N}i} \right] \tag{3}$$

$$C_{\mathrm{E}} = \sum_{t=1}^{T} \sum_{i=1}^{N} \left[\left(\alpha_i + \beta_i P_{\mathrm{G}_{i,t}} + \gamma_i P_{\mathrm{G}_{i,t}}^2 \right) u_{i,t} \right] \tag{4}$$

$$F_{\mathrm{N}i} = \left(a_i P_{\mathrm{G}_{i,t}} + b_i P_{\mathrm{G}_{i,t}} + c_i \right) u_{i,t} \tag{5}$$

where T - scheduling cycle; N - number of fuel generators; α_i, β_i and γ_i - carbon emission coefficients of the generator i respectively; $F_{\mathrm{N}i}$ - fuel cost of unit i; $P_{\mathrm{G}i,t}$ - active power of unit i at period t; a_i, b_i, c_i - power generation cost parameters and $u_{i,t}$ is binary variable which indicates the status of unit i in time t (on = 1, off = 0).

Table 1 Summary of cases

Case	Detail
I	*Grid, D_iG (Existing Case)*
II	*PV (no tracking), Biogas generator (BG), Wind, Battery, Converter*
III	*PV (two-axis tracking), BG, Wind, Battery, Converter*
IV	*PV / Wind, D_iG, Battery, Converter*
V	*PV, BG, D_iG, Wind, Battery, Converter*

After finding the feasible system configuration a sensitivity analysis is performed to check the supply reliability and to perform risk analysis based on the sensitivity parameters. We considered five different cases in order to determine the most promising option for microgrid planning as given in Tab. 1.

3.1 Load

A load profile of a typical industry (Kamal Mills) located at 31°38'0" North latitude and 73°14'0" East longitudes near Faisalabad, Pakistan is considered. We

classified the industrial load into four profiles i.e. the main load, lighting load, deferrable load and thermal load as shown in Fig. 3.
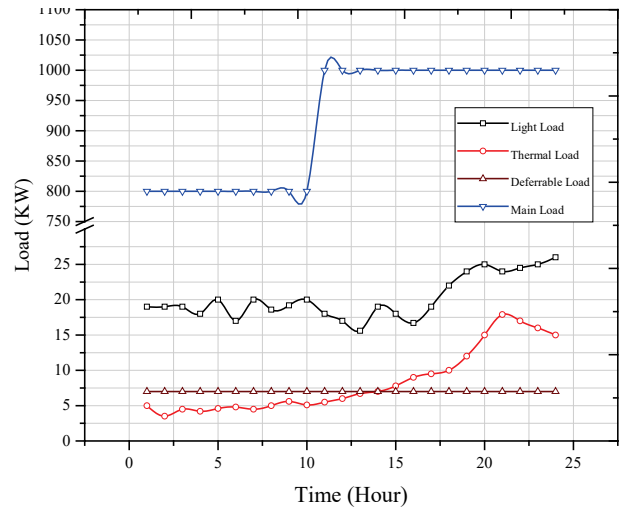

Figure 3 Load profiles

The main load is almost a constant load; it changes only into two-time steps while the lighting load varies over 24 hours. The reason for this step (200 kW) change in the main load profile is turning on an industrial machine load which turns on at 1000 h and remains on till 2400 h. Other load features are given in Tab. 2.

The heat is needed for the different industrial processes. The thermal load can be served by the boiler, by a generator from which waste heat can be recovered, by surplus electricity, or by the solar thermal collector. The current version of HOMER cannot model a solar thermal collector that serves the thermal load, so in this study, the thermal load is served by the boiler and by excess electricity, while the fuel used for the boiler is biodiesel to reduce emissions and cost.

Table 2 Load characteristics

Load Type	Average / kWh/day	Peak / kW	Load Factor / %	Random Variability	
				t_1-t_2	day-day
Main Load	22, 200	1, 000	92.5	-	-
Lighting	517	48.3	44.6	15	20
Deferrable	5	7	-	-	-
Thermal	197	17.9	46.0	15	20

The Load Factor: It is a ratio between the average load and the peak load. It helps to decide about the sizing of the equipment in the Hybrid Microgrid design.

Random Variability: It is the measurement of how much a load profile can vary from one-time interval to next time interval (here time step can be one minute o one hour) and from one day to next day. This factor helps to decide the ratings of the equipment.

3.2 Solar *PV* Model

The output power of a *PV* system can be calculated by its rated output power at the standard test condition, light intensity, and the operating ambient temperature as defined in Eqs. (6) to (8).

$$P_{pv} = P_{pv,STC} \frac{G_c}{G_{STC}} [1 + k(T_c - T_{STC})] \qquad (6)$$

$$0 \leq P_{pv} \leq P_{pv}^{max} \qquad (7)$$

$$\frac{P_{pv}}{S_{pv}} \geq \cos\phi_{max} \qquad (8)$$

- P_{pv} - *PV* output power / kW
- *STC* - the standard test condition (*STC*) means that solar irradiance is W/m, PV temperature is 25 °C, and relative atmospheric optical quality is AM1.5 condition.
- G_C - irradiance of the operating point
- K - power temperature coefficient
- P_{STC} - rated output power under STC
- T_C - *PV* temperature operating point

3.2.1 Solar *PV* Profile

Pakistan is ideally situated in the sun-drenched belt, an average solar global insolation 5-7, kWh/m²/day exists in the country over more than 95% of its areas with persistence factor of over 85% [24, 25]. The solar resource used for current study at a location of 31°38'0" North, 73°14'0" East (Sahiān-wāla, Faisalabad, Punjab, Pakistan, Asia) was taken from NASA Surface Meteorology and Solar Energy website [26].
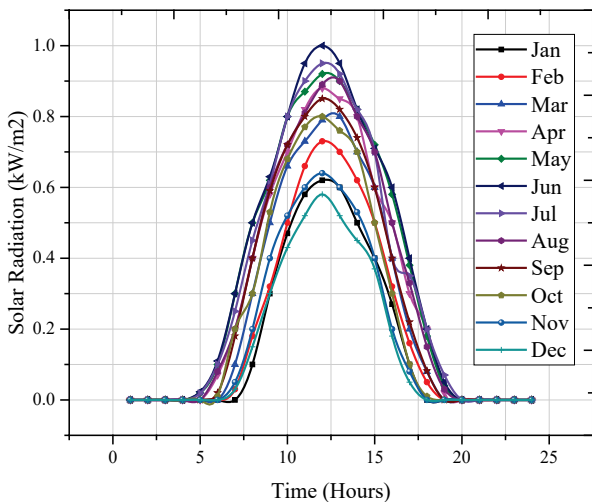

Figure 4 Solar radiation profile

The annual average solar radiation scaled to be 5.19 kWh/m²/day with an average clearness index of 0.64. The solar radiation is available throughout the year; therefore a considerable amount of PV power output can be obtained (see Fig. 4). National Electric Power Regulatory Authority (NEPRA) determined the projected cost for the solar power plant > 1 MW ≤ 20 MW in Pakistan $1 562 770 per MW.

The capital cost includes the PV panels, inverter, design, engineering and management, array structure, shade, fencing, land price shipping, tariffs, installation and dealer mark-ups. We considered two types of PV panels in our study i.e. with and without a tracking system, besides studying their impact on the cost; their technical performance is also investigated. A de-rating factor of 90%

takes into account to cater the varying effects of temperature and dust on the panels. For this study, we considered AZM726P solar panels with the following characteristics $P_{nominal}$ = 310 W, v_{OC} = 46.05 V, I_{SC} = 8.80 A.

3.3 Wind Turbine (WT) Model

The approximate relationship between the output power of wind turbine (WT) and wind speed can be obtained by Eq. (9) and Eq. (10).

$$P_w(v) = \begin{cases} 0 & v \leq v_{ci} \quad \text{or} \quad v \geq v_{co} \\ \dfrac{P_{rated-W}(v - v_{ci})}{(v_r - v_{ci})} & v_{ci} \leq v \leq v_r \\ P_{rated-W} & v_r \leq v \leq v_{co} \end{cases} \qquad (9)$$

$$0 \leq P_w \leq P_{rated-W}^{max} \qquad (10)$$

- v_{ci} - cut-in speed
- v_{co} - cut-off speed
- v_r - rated wind speed
- $P_{rated-W}$ - rated output power of *WT*

3.3.1 Wind Profile

The monthly average resource data from an average of ten years was taken from the NASA website [26] based on the longitude and latitude shown in Fig. 5.
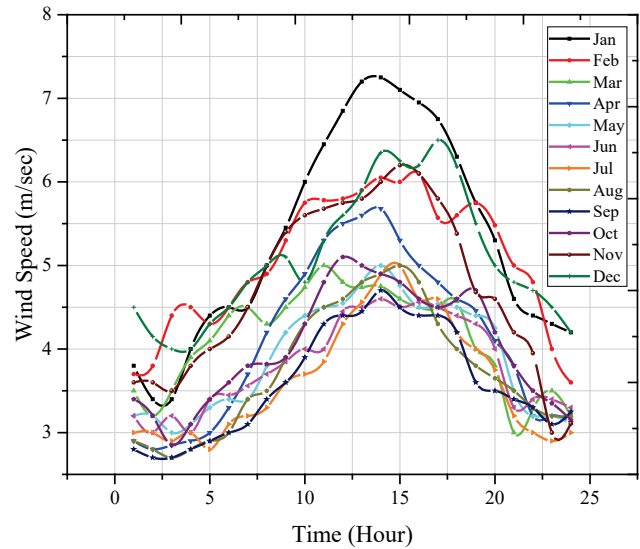

Figure 5 Wind profile

The annual average wind speed for the location is 4.25 m/s at 50 m height. The wind probability and average monthly speed throughout the year are also observed. The wind speed variation over a day is 0.25, the randomness in wind speed (autocorrelation factor) is 0.8, and surface roughness length is 3 m (city centre tall buildings). HOMER fits a Weibull distribution to the wind speed data. As average wind speed is 4.25 m/s so we used GE-50 model wind turbine which is more efficient at these wind speeds considering K = 1.83. The specifications of the

selected wind turbine are: $P_{\text{rated-WT}}$ = 10 kW, output voltage = 240 V_{ac}, v_{ci} = 3 m/s and v_{co} = 10 m/s.

3.4 Wind/Solar Potential

From 900 h to 1800 h a tremendous amount of solar power is available while from 1000 h to 2000 h wind potential is available. Now if we observe load profile (main load) it has a maximum value from 1000 h to 2400 h (1000 kW). So this type of Wind/Solar profile is perfect for an industrial profile. From 1000 h to 2000 h the main load can be served by Wind/Solar potential as shown in Tab. 3.

Table 3 Available Wind/Solar potential vs industrial load profile

Time / h	Load / kW	PV / kW	Wind / kW
00:00-03:00	800	0	116
03:00-06:00	800	0	147
06:00-09:00	800	135	211
09:00-12:00	1000	732	328
12:00-15:00	1000	761	392
15:00-18:00	1000	0	475
18:00-21:00	1000	0	287
21:00-24:00	1000	0	207

3.4 Fuel Generators Model

In this study, we consider two types of fuel generators i.e. biogas generator (*BG*) and diesel generator (*DiG*). Generator serves as a backup especially when there is not enough renewable power available. The fuel consumption (L/kWh) of the generators is modeled as a linear function of their actual output power as shown in Eqs. (11) to (14).

$$C_{\text{bg}} = C_0 \cdot P_{\text{bg\_rated}} + C_1 \cdot P_{\text{bg}} \qquad (11)$$

$$0 \le P_{\text{bg}} \le P_{\text{bg\_rated}}^{\max} \qquad (12)$$

$$C_{\text{DiG}} = C_0 \cdot P_{\text{DiG\_rated}} + C_1 \cdot P_{\text{DiG}} \qquad (13)$$

$$0 \le P_{\text{DiG}} \le P_{\text{DiG\_rated}}^{\max} \qquad (14)$$

- *C* - fuel cost / $/L/kWh

3.5 Biomass Profile

Most common biofuels are bioethanol, biodiesel & biogas. In the present study, we use biodiesel to operate boiler which can serve the thermal load and biogas to generate electricity. The purpose of integrating bioenergy in the study instead of petroleum diesel is to reduce emissions and cost [27]. The raw materials for biogas include agriculture waste, animal dung, municipal waste, plant materials, sewage, green waste etc. Total biogas generation potential of 14.25 million m³/day is available in the country [25, 28].

Biogas usually has a low heating value compared with solid biomass but it has several advantages, including cleaner combustion, higher efficiency, and better control. Fig. 6 shows the available biomass potential at the site.
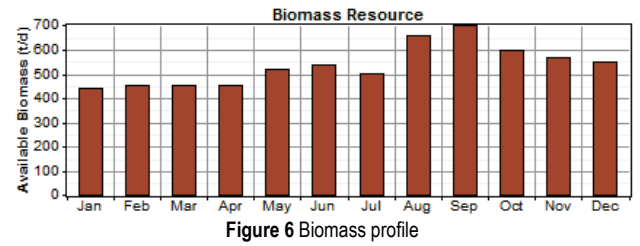
Figure 6 Biomass profile

The characteristics of biogas are: density = 1.22 kg/Nm³; specific gravity = 0.94; calorific value = 4500 Kcal/m³ (17 MJ/m³) amount of gas required to generate 1 kWh of electricity = 0.6 m³; digester size = 50 m³, efficiency = 80%. Biogas has less heating value than the fossil fuel so the ratio with which the biogas replaces fossil fuel in a cofired generator is 8:1. This ratio is assumed to be constant, independent of fuel mixture or output power. The main advantages of biodiesel over petroleum diesel are: biodiesel has only 4% carbon and no sulphur content while petroleum diesel has 88% carbon and 0.33% sulphur contents, and it is also cheaper than petroleum diesel. So under the present circumstances, biodiesel is the best option to be utilized in the present study to operate the boiler that can serve thermal load. The most commonly available biodiesel are B20 (blend of 20% biodiesel + 80% petroleum diesel) and B100 which is pure biodiesel.
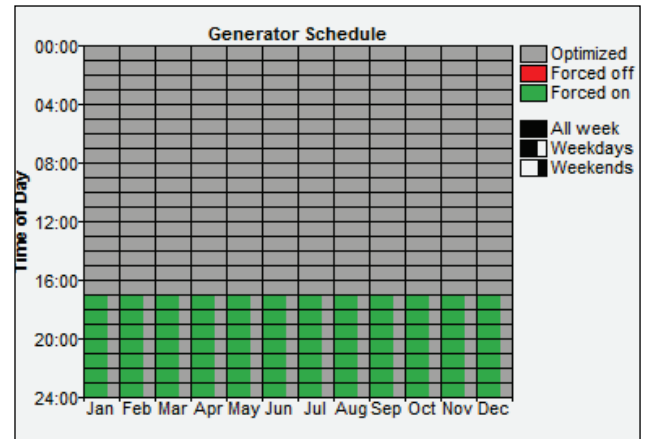
Figure 7 Biogas generator schedule

As it is obvious from the load profiles that the load is maximum from 1800 h to 2400 h except for weekends so we scheduled biogas generator to be forced on during this time slot as shown in Fig. 7. The rest of the week and remaining time slot is left for HOMER to optimize the operation from all available sources. This is done because if this system is considered as a grid-connected system, the purchased rate of energy from the grid during these hours will be high.

3.6 Battery Energy Storage System (BESS) Model

The battery storage system is one of the core parts of the hybrid microgrid system. The strategy of managing the batteries significantly impacts the performance of the overall system. At any given time, the state of charge (*SOC*) of the battery system should be within a certain range defined in Eq. (15) and Eq. (16).

$$SOC_{min} \leq SOC \leq SOC_{max} \qquad (15)$$

$$P_{bat\_c, max} \leq P_{bat} \leq P_{bat\_d, max} \qquad (16)$$

- SOC_{min} - SOC lower limit
- SOC_{max} - SOC upper limit
- $P_{bat\_c, max}$ - maximum allowed charge power
- $P_{bat\_d, max}$ - maximum allowed discharge power

The value of SOC at time $t + \Delta t$ can be determined by the value of SOC at time t and the battery power P_{bat} during this time period by using Eq. (17). The SOC should be controlled within the range defined in Eq. (15).

$$SOC_{t+\Delta t} = SOC(t) - P_{bat}(t) \cdot \frac{\Delta t}{C_{bat}} \qquad (17)$$

- C_{bat} - capacity of the battery

Batteries provide an operating reserve in the system and keep the voltage constant through peak load hours or in case of shortfall in the generation capacity especially in night hours when there is no solar energy available. "Spinning reserve" is a more common term that means precisely the same as an operating reserve. We call it operating reserve simply because batteries, fuel cells, and the grid can provide it, but they do not spin. The battery selected for this study is Surrette 4KS25P deep cycle lead-acid battery. It is a 4 V battery with a nominal capacity of 1900 Ah (7.6 kWh).

The maximum capacity (or theoretical capacity) of a battery is the total amount of energy it holds when completely charged. It is not possible to extract all this energy at any finite discharge current so battery sizes are not usually given in terms of maximum capacity. HOMER calculates the maximum capacity for use in the kinetic battery model. HOMER allows setting the DC bus voltage by defining a number of batteries per string. We considered 12 batteries per string in our study to make a 48-volt DC bus. HOMER models the batteries on charging and discharging cycle.

3.7 Economic Model for Hybrid Microgrid System

The Levelized cost of energy (*LCOE*) and net present cost (*NPC*) are principle economic factors to rank various system configurations. HOMER defines the *LCOE* as the average cost per kWh of useful electrical energy produced by the system as illustrated in Eq. (18).

$$LCOE = \frac{C_{ann,tot} - C_{boiler} E_{thermal}}{E_{primary,AC} + E_{def}} \qquad (18)$$

- $C_{ann, tot}$ - total annualized cost of the system / \$/y
- C_{boiler} - boiler marginal cost / \$/kWh
- $E_{thermal}$ - total thermal load served / kWh/y
- $E_{prim, AC}$ - total primary AC load served / kWh/y
- E_{def} - deferrable load served / kWh/y

The total annualized cost is equal to its annual operating cost plus capital and replacement costs over the

project lifetime. The total net present cost (*TNPC*) is HOMER's main economic output. HOMER ranks all systems according to *TNPC*. The *TNPC* of a system is the present value of all the costs that it incurs over its lifetime, minus the present value of all the revenue that it receives over its lifetime as illustrated in Eq. (19). Costs include capital costs, replacement costs, *O&M* costs, fuel costs, and emissions penalties.

$$TNPC = \frac{C_{ann,tot}}{CRF(i, N)} \qquad (19)$$

$$CRF = \frac{i(1+i)^N}{i(1+i)^N - 1} \qquad (20)$$

- $CRF(i, N)$ - the capital recovery factor
- i - interest rate
- N - the project lifetime / year(s)

Economics inputs considered in this paper are as follows:
- annual interest rate = 6%
- project lifetime = 25 years
- system fixed capital cost = 0 \$
- system fixed O&M cost = 0 \$
- capacity shortage penalty = 0 \$/kWh

HOMER applies these economic inputs to each system to calculate the system's NPC. The input sizes, capital cost and operation and maintenance (*O&M*) cost that are considered for this study are given in Tab. 4.

Table 4 Sizing options and cost

Sources	Sizes	Capital cost	O&M cost
DiG / kW	0-1500	350 \$/kW	0.03 \$/h/kW
PV / kW	1-3500	1500 & 2000 \$/kW	0 & 15 \$/y/kW
WT / no	10-20	8000 \$/turbine	30 \$/y/turbine
BG / kW	0-800	1000 \$/kW	0.03 \$/h/kW
Battery / string	0-200	150 \$/battery	10 \$/y/battery
Convertor / kW	0-2500	350 \$/kW	0

3.8 Operation Strategy

The controller can be designed very easily in HOMER as shown in Fig. 8. First write the code in C++ or in MATLAB then run and test it, if the code is ok then compile this code into a .dll file and distribute into HOMER controller option. The other option to design controller is by setting parameters in the software. The operation strategy is defined for 24 hours for every minute as shown in Fig. 9. In the daytime, the role of BESS is fast frequency control, i.e. balancing the sudden variation in the output in renewable sources especially wind and *PV* in this case. It is otherwise kept idling, in order to reduce battery ageing as much as possible. Operation strategy must fullfill the power balance constraint defined in Eq. (2). The target BESS *SOC* is 80%, i.e. 15 minutes charge/discharge at rated power, which is abundantly compatible with the start-up time of diesel and biogas generators. The BESS is charged (up to 80% *SOC*) when renewable's output exceeds the total demand. Algorithm for operation strategy is shown below.

```
      for(t = 1, t < 1440, t++)
if((Ppv + PW + Pbg > PN-Load)&&(SOC <80))
Pbat = Ppv + PWT + Pbg -PN-Load;
else if((Ppv + PW + Pbg>PN-Load)&&(SOC>=80))
            PEE = Ppv + PW + Pbg - PN-Load;
            PF-Load = PEE;
else if((Ppv + PW + Pbg<PNLoad)&&(SOC>=20))
            PN-Load = Ppv +PWT + Pbg + Pbat;
else if(Ppv + PW +Pbg < PN-Load)&&(SOC <20)
PN-Load = Ppv + PW + Pbg + PDiG;
      Pbat= Ppv + PW + Pbg + PDiG -PN-Load;
else
            Ppv + PWT + Pbg = PN-Load;
```

- P_{N-Load} - non flexible load
- P_{EE} - excess electricity
- P_{F-Load} - flexible load
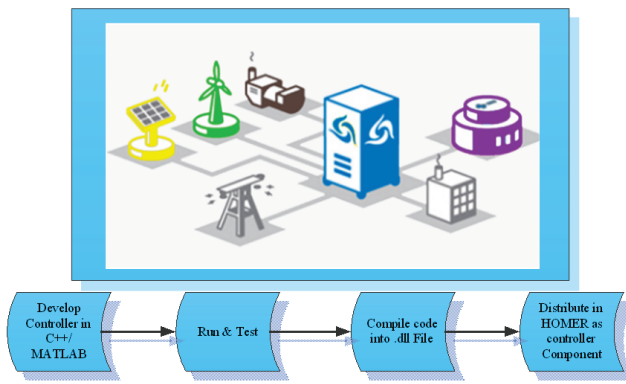- P_{bat} - battery power
- P_{T-Load} - thermal load

Figure 8 HOMER controller option

4 SIMULATION & RESULTS

The simulation capability of HOMER is the long-term operation of the microgrid. The optimization and sensitivity analysis of HOMER depends on this simulation capability [29]. Fig. 10 shows the available portfolio of RETs in microgrid planning that is considered in case II, III, IV & V, while case-I is the existing scenario (Grid-D_iG). Case-II considers the *PV* panels with fix angle (slope = 31.633 W to S), wind, batteries, converter Biogas generator (*BG*). Case-III has the same combination as case-II but solar panels are considered with a two-axis tracking system to harness maximum solar energy. The panels are rotated about both horizontal and vertical axes so that the sun rays are always perpendicular to the surface. Case-IV includes D_iG instead of *BG* and finally, case-V is the combination of case III & case IV. System optimal sizing is presented in Tab. 5.

Table 5 Optimal microgrid plan for different configurations

CASE#	I	II	III	IV	V
DiG / kW	1000	0	0	1000	10
Grid / kW	500	0	0	0	0
PV / kW	0	3000	2500	2000	2500
WT / no	0	20	20	20	20
BG / kW	0	800	800	0	800
Battery / no	0	2400	2400	1200	2400
Convertor / kW	0	1500	1200	1000	1200

4.1 Optimization Method

HOMER adopts enumeration method to simulate all possible schemes defined. After simulating all of the possible system configurations, HOMER displays a list of configurations, sorted by net present cost (sometimes called lifecycle cost), that we can use to compare system design options. For optimization, model HOMER needs decision variables sometimes also called optimization variables. A decision variable is a variable whose optimal value is determined during the course of the optimization process. Here decision variables are: size of the *PV* array, number of wind turbines, size of each generator, number of batteries, size of the converter and dispatch strategy.

4.2 Constraints and Control Parameters

HOMER allows its user to set constraints and control parameters that are very helpful while designing a hybrid system. It is considered that the proposed system must be able to produce a minimum 60% renewable energy of the total electric energy consumed, which is a user-specified constraint and depends on system design. This value can be varied as per user choice and causes a remarkable impact on the TNPC. Similarly, one more constraint imposed during the simulation process is the maximum annual capacity shortage. This parameter is set at "0" as the industry cannot compromise with reliability or interruption in the energy supply. With this assumption, the system configuration is estimated that the system is able to supply the peak load, which even occurs for a short period of time. Other constraints and control parameters considered in this work are as follows:

- Operating reserve from *PV* output = 30%
- Simulation time step = 1 hour
- Setpoint state of charge = 80%
- Allow system with generator less than peak load
- Allow excess electricity to serve thermal load.

4.3 Comparative Analysis

Case-V has least *TNPC*, *COE* and operating (Opr.) cost as shown in Tab. 6. But case-V has slightly more emissions than case-II & Case-III (see Tab. 7).

Table 6 Costs comparison of different configurations

CASE#	I	II	III	IV	V
TNPC / M$	39.87	12.30	13.85	29.39	10.31
COE / $/kWh	0.375	0.115	0.129	0.365	0.096
O&M / M$/y	3.10	0.460	0.468	2.75	0.473

Table 7 Pollutant emission comparison of different configurations

kg/y	I	II	III	IV	V
CO_2	11 482 169	17 843	15 594	9 183 341	32 792
CO	21 453	19.2	17.2	22 622	54.9
SO_2	29 501	83.9	73.3	18 494	112
NO	197 297	162	145	201 861	482

Case-II has less *TNPC*, operating cost and *COE* than case-III because in case-III solar tracking system adds an additional cost. But on the other hand case-III generates more output from *PV* even with the same sizing of *PV* panels among all the cases, because tracking system maximizes the efficiency of *PV* panels (see Tab. 8).

Considering a tracking system for the *PV* array can obtain 52.13% more energy which is much better as compared to system discussed in [22, 23].

Case-II is considered with fix angle *PV* pannels while Case-III, IV & V are considered with two axis tracking system. The case-IV (*Wind-PV-Battery-DiG-Converter*) still has *COE* less than the existing case and also with reduced emissions, which clarifies the feasibility of the proposed system.

Jan Shair [30] found that *PV, DiG, Battery, Converter* architecture is the most economical system for a technical college load having *COE* 0.159 $/kWh. Omar Hafez [16] found *DiG, Wind, PV, Battery, Micro-hydro, Converter* is

the most feasible option for a rural community load having *COE* 0.278 $/kWh.

While Asad Waqar [17]] projected a microgrid consisting hydro turbine, biomass generator, diesel generator, PV array and batteries to find out the optimal system outline in terms of generation mix and unit sizing with minimum costs (*NPC* = 6.80 M$, *COE* = 0.045 $/kWh).

Tab. 6 shows that the proposed system has more promising results due to the integration of more RETs and with proper use of excess electricity. All the cases considered in this study are found feasible and economical compared to the existing scenario and with previous literature.
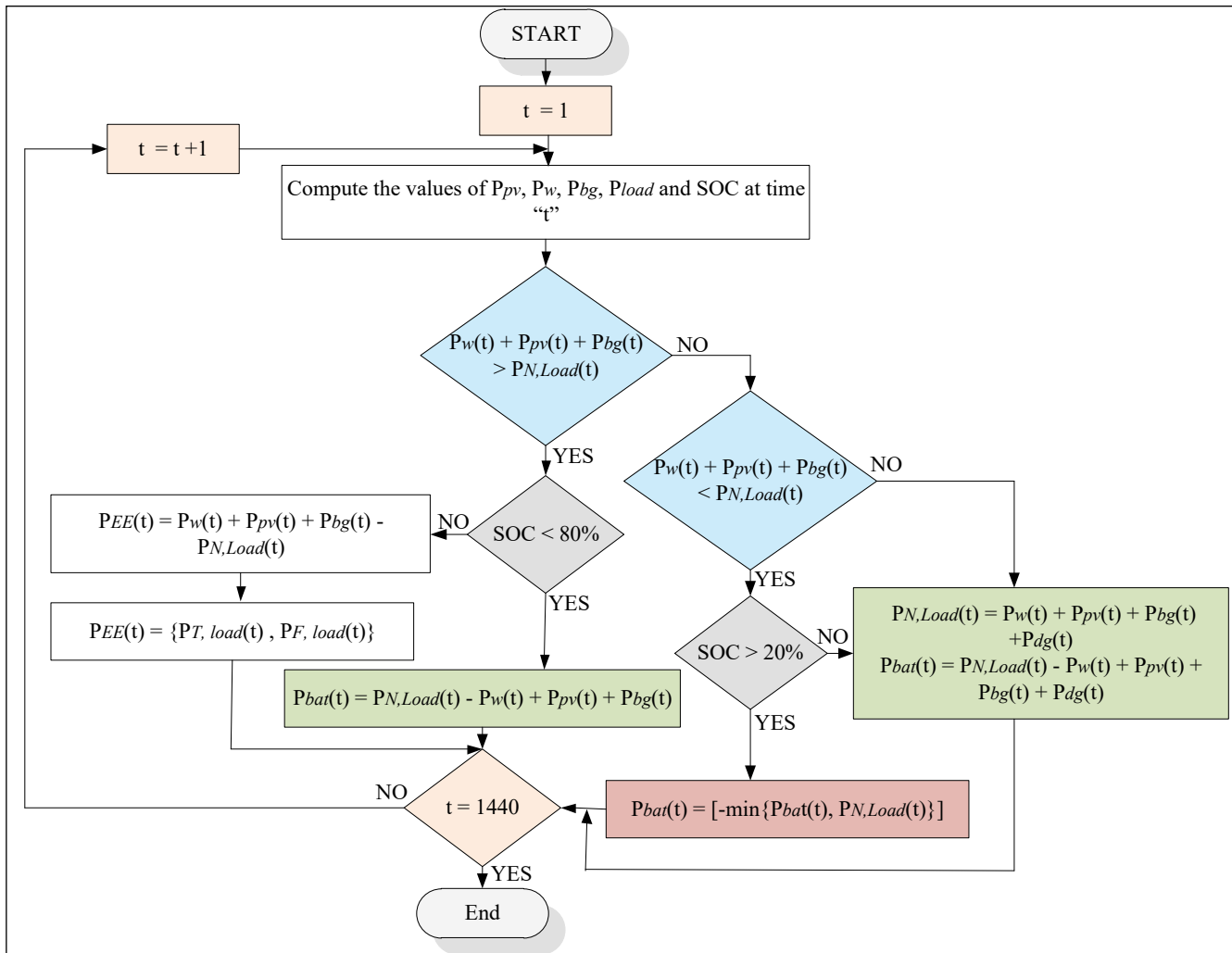

Figure 9 Operation strategy ($P_{T, load}$ = Thermal Load; $P_{F, load}$ = Flexible Load; P_{bg} = Output Power of Biogas Generator; P_{dg} = Output Power of Diesel Generator; $P_{N, Load}$ = Non-flexible Load; P_{bat} = Battery Power; P_{EE} = Excess Electricity; SOC = State of Charge (battery))

4.4 Savings and CO$_2$ Reduction

The annual average load is 30,06,687 kWh, and with the current rate of *COE* (0.375 $/kWh) the user has to pay 11,27,512 $ annually for the energy he consumed. If we compare the existing case with the proposed system (case-V) which has the *COE* of 0.096 $/kWh, a user can save up to 74% of his cost every year and with this rate of saving user can pay back the capital cost of the new system (Case-V: *TNPC* = 10.31 M$) in 12.3 years. Similarly, CO$_2$ is reduced up to 99.71% as shown in Tab. 7.

Table 8 *PV* with fix angle vs two axis tracking system

	I	II	III	IV	V
PV Maximum output / kW	0	397	761	467	672
Excess Electricity / %	0	9.53	18.2	3.36	9.05
T - load served by EE / %	0	94	97	83	92
Renewable Fraction / RF	0	100	100	44.9	97.3

HOMER allows to use excess electricity to serve thermal load as shown in Tab. 8 i.e. % thermal load served by excess electricity. Fig. 11 shows the percentage contribution from all the available sources.
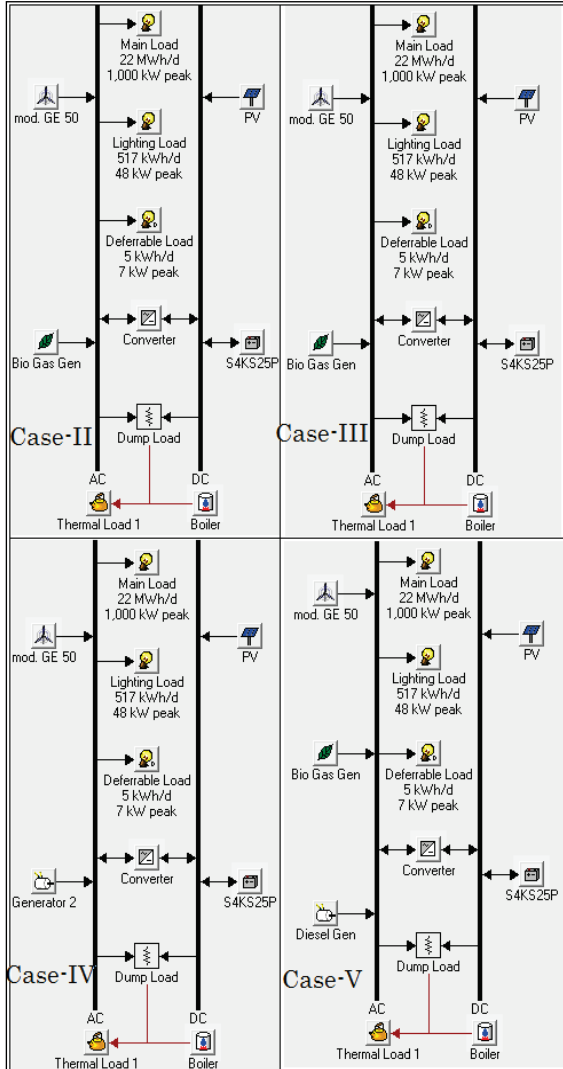
Table 9 Sensitivity parameters

Parameter	Sensitivity Values
Diesel price / \$/L	0.6, 0.8
Scaled annual average *PV* isolation / kWh/m²/d	5.19, 4.0
Scaled annual average wind speed / m/s	4.25, 3
Biodiesel price / \$/L	0.4, 0.6
Scaled annual average Biomass / ton/d	550, 300
Interest rate / %	0.6, 0.5

Figure 10 Available portfolios of energy options in microgrid planning

Figure 11 Percentage contribution of available sources

4.5 Sensitivity Analysis

The main objective of using the sensitivity analysis in HOMER is that if the user is not sure about the optimal value of a certain variable, then the user can enter different values and can witness the behaviour of the results. The vital variables for the microgrid system are often tentative. This is a key problem to be overcome while designing the system.

In present study sensitivity parameters are wind average speed, solar insolation, diesel price, Biodiesel price, biomass production and interest rate, the corresponding values are shown in Tab. 9, the bold and italic values are the base values and others are sensitivity values. A user can take some random values and can observe the behaviour of the system against those values, i.e. user can observe which are the parameters that have more effect on the system in terms of sensitivity, system reliability and stability.

Tab. 10 and Tab. 11 show that all the cases except case I & IV have stable results against sensitivity parameters. Sensitivity parameters are first varied separately then varied with different combinations to observe their effect on the system clearly.

Table 10 Optimal sizing after sensitivity analysis

Sources	I	II	III	IV	V
D_iG / kW	1000	0	0	1000	0
Grid / kW	500	0	0	0	0
PV / kW	0	2500	2000	2000	3000
Wind / no	0	20	20	20	20
Battery / no	0	2400	2400	1200	2400
BG / kW	0	800	800	0	800
Converter / kW	0	1500	1300	1300	1500

Table 11 Cost comparison after sensitivity analysis

| Cost	I	II	III	IV	V
TNPC / M\$	44.10	11.59	11.93	42.10	11.75
COE / \$/kWh	0.415	0.108	0.111	0.355	0.110
O&M / M\$/y	3.45	0.462	0.470	2.96	0.417

4.6 Supply Reliability

Junbio Han proposed an intelligent control algorithm for a microgrid with multiple renewable resources that aims at maintaining the smart grid at the optimum operating point under various operating conditions such as load variation, insolation change, wind speed change etc [31]. To check the system supply reliability we tested all the cases against load variation i.e. 10% increase in the main load, with 10% increase in load, daily demand is increased to 24 MWh and peak load is increased to 1100 kW.

Table 12 Cost comparison after sensitivity analysis

Case	Dispatch strategy	Feasibility	COE / \$/kWh
I	Load Following	Yes	0.413
II	n/a	No	n/a
III	n/a	No	n/a
IV	Cycle charging	Yes	0.378
V	Cycle charging		0.107
	Load Following	Yes	0.187

Tab. 12 represents the results after 10% increase in load, there is no feasible solution for case-II and case-III due to capacity shortage constraint while case-V is found feasible
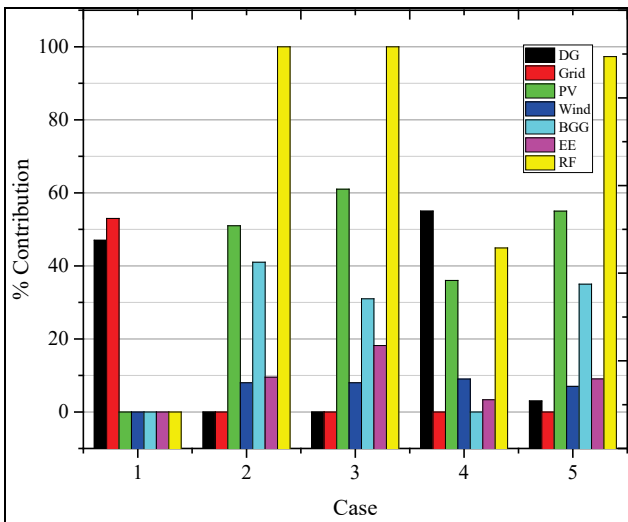
and more economical as compared to all cases. Case-V has two feasible solutions with two types of dispatch strategies; 1) Cycle charging (CC) which includes batteries and 2) load following (LF) which is without batteries.

4.7 Battery State of Charge (*SOC*)

When *SOC* is below the set point and the battery was not discharging in the previous hour, HOMER will avoid discharging the battery in this hour. A generator will likely be called upon to serve the primary load and produce excess electricity to charge the battery bank. So once the system starts charging the battery bank it continues to do so until it reaches the set point state of *SOC*. The setpoint of *SOC* tends to decrease the time that battery bank takes at a low *SOC*. It also tends to reduce the number of generator starts and the number of battery charge-discharge cycles that take place throughout the year. The setpoint of *SOC* in the under discussion system is set to 80%.
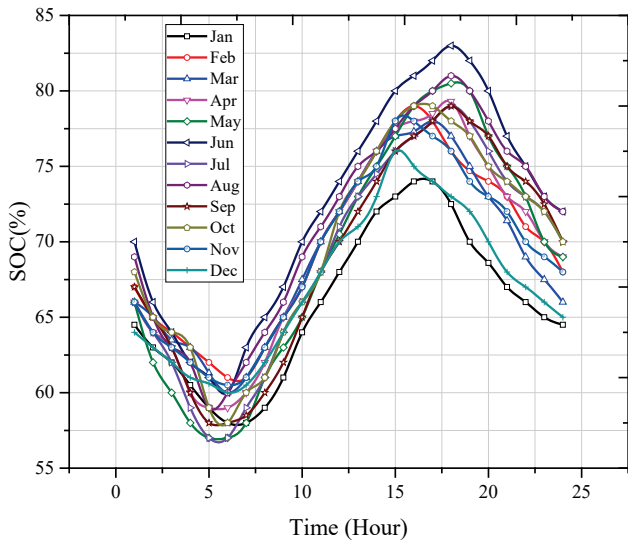

Figure 12 Daily battery *SOC* over a year (case-V)

The target *SOC* is 50%, i.e. 15 minutes charge/discharge at rated power, which is abundantly compatible with the start-up time of backup diesel and biofuel generator. The BESS is charged (up to 80% *SOC*) when Renewable output exceeds the total load demand, according to the conditions defined in Eq. (21).

$$\text{If } \left(\{P_{pv}(t) + P_w(t) + P_{bg}(t)\} > P_{\text{N-Load}}(t) \, \& \, SOC(t) < 80\% \right)$$
then (21)

$$P_{\text{battery}}(t) = \left(P_{pv}(t) + P_w(t) + P_{bg}(t) - P_{\text{N-Load}}(t) \right)$$

where $P_{\text{battery}}(t)$ is the power drawn by the BESS (+ve when charging) at time *t*. In case *PV* output exceeds total load despite full battery utilization, *PV* operating mode is switched from Maximum Power Point Tracking (MPPT) to Required Power Point Tracking (RPPT), thus reducing the *PV* output. Fig. 12 shows the daily battery *SOC* of case-V for all the months of the year. It is clear from the Fig. 12 that *SOC* follows the specific pattern all over the year i.e. it follows the proposed operation strategy.

4.8 System Operation

Fig. 13 shows the operation of the system for 24 hours for all sources, battery *SOC*, Primary load served. It is obvious from Fig. 13 that in the day time when there is enough renewable energy available, fuel generators remain off. Fuel generators call upon in the night hours and in the morning when there is not enough renewable energy available and during these hours load is served by the biofuel generator and battery power. Batteries also provide the spinning reserve, which compensates the uncertainties in the wind and *PV* and also takes care of load variations.
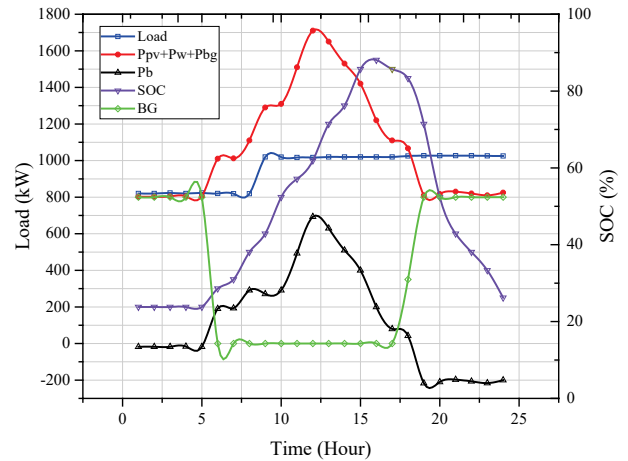

Figure 13 System operations for 24 hours [P_b = battery power, $P_w + P_{pv} + P_{bg}$ = wind, *PV* and biogas generator combine output, *Load* = main load, *BG* = biogas generator operation]

Fig. 14 shows how the proposed system uses the excess electricity to serve thermal load, to operate the boiler and to charge batteries. After serving the main load (non-flexible load) if there is enough renewable potential available it would be harnessed and generate excess electricity than system requirements. This excess electricity can be used for different purposes so in this system efficiency will definitely be increased and allow the system to utilize the available sources more effectively. A random time period (first week of June) is selected to explain the operation of the system.
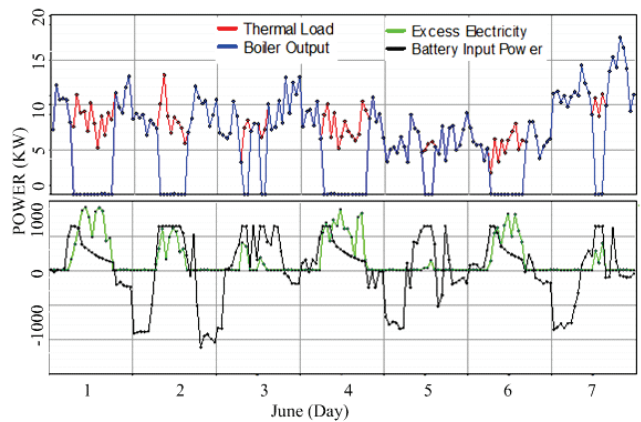

Figure 14 Use of excess electricity according to defined operation strategy [red line = thermal load, blue line = boiler output, green line = excess electricity, black line = battery input power (+ve = charging, −ve = discharging)]

To serve the thermal load the first priority is given to excess electricity if it is available at that time otherwise it

will be served by the boiler as shown in Fig. 14. When there is excess electricity available the thermal load is served by the excess electricity and boiler remains off during that time period. Moreover, if the excess electricity is more than the thermal load requirements it also charges the batteries if the battery *SOC* is less than 80% during that time period.

5 CONCLUSIONS

This paper explored a methodology for optimal sizing of a hybrid energy system for an industrial load using HOMER with improved topology. Technical feasibility and lifecycle costs of a microgrid for each hour of the year are determined using HOMER. In addition, the microgrid configuration and operation strategy of the supply components are tested to examine how these components work in a given setting over a period of time. Different possible cases are considered in this study and operational strategy is proposed which not only considers the battery *SOC* to improve battery's life but also to improve overall system efficiency. Finally, the optimal sizing method is applied to find out the optimal configuration. It is perceived from the obtained results that *PV-BG-D$_i$G-Wind-Batteries-Convertor* hybrid system is a cost-effective and feasible solution in terms of *COE* and *NPC*. Moreover, the proposed system is tested for supply reliability by increasing the 10% load demand and by applying the capacity shortage constraint. Dispatch strategy plays an important role especially while considering the system supply reliability taken into account. *PV* system with and without tracking system is considered in this study in a microgrid context and has remarkable results as compared to previous literature which only studied this comparison as a separate system. It is found that by using PV tracking system in a microgrid system it can increase its output power more as compared to a separate system.

Further if industries adopt this proposed system it will lead to overcoming the energy crisis in Pakistan. If this proposed system is implemented it will not only provide the reliable and environment-friendly energy to the industries at a reasonable cost but it will also relieve the burden on the national grid.

6 REFERENCES

[1] Qasim, M. & Kotani, K. (2014). An empirical analysis of energy shortage in Pakistan. *Asia-Pacific Development Journal, 21*,137-166. https://doi.org/10.18356/e84bd5d1-en
[2] Shakeel, S. R. et al. (2016). Renewable energy sources in power generation in Pakistan. *Renewable and Sustainable Energy Reviews, 64*, 421-434. https://doi.org/10.1016/j.rser.2016.06.016
[3] Amer, M. & Daim, T. U. (2011). Selection of renewable energy technologies for a developing county: a case of Pakistan. *Energy for Sustainable Development, 15*, 420-435. https://doi.org/10.1016/j.esd.2011.09.001
[4] Stevanoni, C., Vallee, F., De Greve, Z., & Deblecker, O. (2017). On the use of game theory to study the planning and profitability of industrial microgrids connected to the distribution network. *CIRED-Open Access Proceedings Journal, 2017*(1), 2444-2448. https://doi.org/10.1049/oap-cired.2017.0394
[5] Choobineh, M., Silva-Ortiz, D., & Mohagheghi, S. (2018). An Automation Scheme for Emergency Operation of a Multi-Microgrid Industrial Park. *IEEETransactions on Industry Applications, 54*(6), 6450-6459. https://doi.org/10.1109/TIA.2018.2851210
[6] R. M. Kamel, et al. (2010). RETRACTED: Wind power smoothing using fuzzy logic pitch controller and energy capacitor system for improvement micro-grid performance in islanding mode. ed: Elsevier. https://doi.org/10.1016/j.energy.2010.01.030
[7] Tasdighi, M. et al. (2014). Residential microgrid scheduling based on smart meters data and temperature dependent thermal load modeling. *IEEE Transactions on Smart Grid, 5*, 349-357. https://doi.org/10.1109/TSG.2013.2261829
[8] Bidram, A. & Davoudi, A. (2012). Hierarchical structure of microgrids control system. *IEEE Transactions on Smart Grid, 3*, 1963-1976. https://doi.org/10.1109/TSG.2012.2197425
[9] Iyer, S. V. et al. (2010). A generalized computational method to determine stability of a multi-inverter microgrid. *IEEE Transactions on Power Electronics, 25*, 2420-2432. https://doi.org/10.1109/TPEL.2010.2048720
[10] Ustun, T. S. et al. (2013). Fault current coefficient and time delay assignment for microgrid protection system with central protection unit. *IEEE Transactions on Power Systems, 28*, 598-606. https://doi.org/10.1109/TPWRS.2012.2214489
[11] Piagi, P. & Lasseter, R. H. (2001). *Industrial application of microgrids*. Power System Engineering Research Center, University of Wisconsin-Madison,
[12] Starfelt, F. & Yan, J. (2008). Case study of energy systems with gas turbine cogeneration technology for an eco-industrial park. *International Journal of Energy Research, 32*, 1128-1135, https://doi.org/10.1002/er.1450
[13] Momeneh, A. et al. (2016). Design and control of a small-scale industrial microgrid in islanding mode. *Industrial Electronics Society, IECON 2016-42nd Annual Conference of the IEEE*, 72-77. https://doi.org/10.1109/IECON.2016.7793490
[14] Sinha, S. & Chandel, S. (2014). Review of software tools for hybrid renewable energy systems. *Renewable and Sustainable Energy Reviews, 32*, 192-205. https://doi.org/10.1016/j.rser.2014.01.035
[15] Givler, T. & Lilienthal, P. (2005). *Using HOMER® software*. NREL'S Micropower Optimization Model, to Explore the Role of Gen-sets in Small Solar Power Systems Case Study: Sri Lanka. https://doi.org/10.2172/15016073
[16] Hafez, O. & Bhattacharya, K. (2012). Optimal planning and design of a renewable energy based supply system for microgrids. *Renewable Energy, 45*, 7-15. https://doi.org/10.1016/j.renene.2012.01.087
[17] Waqar, A. et al. (2015). Generation Expansion Planning and Evaluation in the Context of Microgrids Using HOMER. *Advanced Materials Research*, 424-428. https://doi.org/10.4028/www.scientific.net/AMR.1092-1093.424
[18] Nasir, M. & Khan, H. A. (2016). *Solar photovoltaic integrated building scale hybrid AC/DC microgrid*. https://doi.org/10.1049/cp.2016.0528
[19] Abbas, M. K. (2015). Economic power generation for an off-grid site in Pakistan. *Power Generation System and Renewable Energy Technologies (PGSRET), 2015*, 1-6. https://doi.org/10.1109/PGSRET.2015.7312189
[20] Zhang, J. et al. (2015). A bi-level program for the planning of an islanded microgrid including CAES. *Industry Applications Society Annual Meeting, 2015 IEEE, 2015*, 1-8. https://doi.org/10.1109/IAS.2015.7356783

[21] Cotto, S. V. & Lee, W. J. (2017). Microgrid Modular Design for Tribal Healthcare Facilities: Kayenta Health Center PV System Case Study. *IEEE Transactions on Industry Applications, 53*, 5121-5129. https://doi.org/10.1109/TIA.2017.2725818

[22] Mamta, S., Singh, G. K. & Saini, R. P. (2013). *Performance evaluation of sun tracking photovoltaic systems*. Case study, 328-335. https://doi.org/10.1049/cp.2013.2193

[23] Mane, S. G., Korachagaon, I., Hans, M. R., & Sawant, A. S. (2018, August). Simulation of Dual Axis Solar Tracking System. *2018 International Conference on Information, Communication, Engineering and Technology (ICICET),* 1-5. https://doi.org/10.1109/ICICET.2018.8533760

[24] Shamshad. K. (1998). Solar insolation over Pakistan. *J SES (Taiyo Enerugi), 24*, 30.

[25] Sheikh, M. A. (2009). Renewable energy resource potential in Pakistan. *Renewable and Sustainable Energy Reviews, 13*, 2696-2702. https://doi.org/10.1016/j.rser.2009.06.029

[26] See https://eosweb.larc.nasa.gov/cgi-bin/sse/sse.cgi

[27] Ilyas, S. Z. (2006). Biogas support program is a reason for its success in Pakistan. *American-Eurasian Journal of Scientific Research, 1*, 42-45.

[28] Ghaffar, M. A. (1995). The energy supply situation in the rural sector of Pakistan and the potential of renewable energy technologies. *Renewable energy, 6*, 941-976. https://doi.org/10.1016/0960-1481(94)00034-0

[29] Lambert, T. et al. (2006). Micropower system modeling with HOMER. *Integration of alternative sources of energy*, 379-418. https://doi.org/10.1002/0471755621.ch15

[30] Shair J. & Abbas, M. K. (2016). Economic viability of grid tied solar PV energy system in Muzaffargarh, Pakistan. *Multi-Topic Conference (INMIC), 2016 19th International, 2016*, 1-6. https://doi.org/10.1109/INMIC.2016.7840149

[31] Han, J. et al. (2015). Adaptive critic design-based dynamic stochastic optimal control design for a microgrid with multiple renewable resources. *IEEE transactions on smart grid, 6*, 2694-2703. https://doi.org/10.1109/TSG.2015.2428435

Contact information:

Zahid JAVID, MS Scholar (S'17)
School of Electrical Engineering Shandong University China,
Jinan, Shandong 250061, P. R. China
E-mail: Zaifuu4444@gmail.com

Ke-Jun LI, Professor (M'07-SM'15)
(Corresponding author)
School of Electrical Engineering Shandong University China,
Jinan, Shandong 250061, P. R. China
E-mail: lkjun@sdu.edu.cn

Rizwan UL HASSAN, PhD Scholar
School of Electrical Engineering Shandong University China,
Jinan, Shandong 250061, P. R. China
E-mail: engr.rizwanulhassan@iefr.edu.pk

Jian CHEN, Lecturer
School of Electrical Engineering Shandong University China,
Jinan, Shandong 250061, P. R. China
E-mail: ejchen@sdu.edu.cn